NASA TECHNICAL NOTE

NASA TN D-3229

NASA TN D-3229

SEMICLASSICAL APPROACH TO CAPTURE COLLISIONS BETWEEN IONS AND POLAR MOLECULES

by John V. Dugan, Jr., and John L. Magee

Lewis Research Center

Cleveland, Ohio

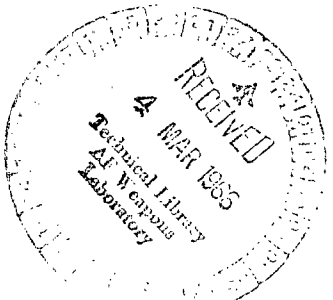

NATIONAL AERONAUTICS AND SPACE ADMINISTRATION • WASHINGTON, D. C. • FEBRUARY 1966

NASA TN D-3229

SEMICLASSICAL APPROACH TO CAPTURE COLLISIONS BETWEEN IONS AND POLAR MOLECULES

By John V. Dugan, Jr., and John L. Magee

Lewis Research Center
Cleveland, Ohio

NATIONAL AERONAUTICS AND SPACE ADMINISTRATION

For sale by the Clearinghouse for Federal Scientific and Technical Information
Springfield, Virginia 22151 – Price $2.00

SEMICLASSICAL APPROACH TO CAPTURE COLLISIONS BETWEEN IONS AND POLAR MOLECULES[1]

by John V. Dugan, Jr. and John L. Magee[2]

Lewis Research Center

SUMMARY

Quantum mechanical average cross sections are derived for low velocity capture collisions between ions and polar molecules. These cross section expressions incorporate the rotational energy of the molecule and are derived from the Stark interaction potential.

A classical upper limit which is good for all ion velocities is presented for the capture cross section. Also, an approximate cross section is derived from classical considerations for the regime of high ion velocity by simple averaging over the static orientations of the polar molecule.

Finally, a numerical calculation of the capture cross section is performed by randomizing initial conditions for two hypothetical molecules with fixed rotational energy at high values of ion velocity. The Lagrangian equations of motion are solved to obtain the capture cross section from a collision ratio. These cross sections are decreasing functions of molecular rotational energy and ion-molecule relative energy. The cross sections are discussed in the context of experimental results and the quantum theoretical predictions.

This study of collision between hypothetical molecular species is intended to serve as a preliminary description of such events.

---

[1]A brief summary of some of the results in this report was given at the 17th Annual Gaseous Electronics Conference, Atlantic City, New Jersey, Oct. 14-16, 1964 and at the 4th International Conference on the Physics of Electronic Collisions at Quebec City, Canada, Aug. 2-6, 1965. More extensive details concerning aspects of this report are included in "A Semi-Classical Theory of Capture Collisions between Ions and Polar Molecules," John V. Dugan, Jr., Ph. D. Thesis, Dept. of Chemistry, Univ. of Notre Dame, Notre Dame, Ind., May 1, 1965.

[2]Professor of Chemistry and Associate Director of Radiation Laboratory, Dept. of Chemistry, Univ. of Notre Dame, Notre Dame, Ind.

INTRODUCTION

The attractive ion-molecule (IM) collision has been extensively studied because of its proposed role in the reaction mechanisms of irradiated gases (ref. 1). Most cross section data for specific IM collisions have come from mass spectrometric experiments. These investigations differ from conventional crossed beam experiments in that average cross sections are measured rather than monoenergetic quantities. The observed cross section Q is a function of the ion energy ϵ_1 which is proportional to a distance ℓ through the target gas (ref. 2). The capture cross section is not measured directly but has a lower limit set by the value of the reaction cross section (ref. 3).

Until recently, the theory employed to calculate IM capture cross sections was identical to that used to describe ion-atom collisions (ref. 4). The Langevin polarization potential

$$V_L = \frac{-\alpha_o e^2}{2R^4} \tag{1}$$

had been used to predict the cross section. This potential term describes the interaction between an ion and the dipole which it induces in the electronic cloud of the molecule (ref. 5). In equation (1), α_o is the average electronic polarizability of the molecule, e the electronic charge, and R the distance between ion and molecule. (A complete list of symbols is included in appendix A.) The cross section for capture was calculated from the equations for conservation of energy and angular momentum. For an IM relative energy ϵ (at infinite distance), the Langevin cross section is (ref. 5)

$$\sigma_L = \pi\left(\frac{2\alpha_o e^2}{\epsilon}\right)^{1/2} \tag{2}$$

The Langevin theory has proven inadequate in predicting the capture cross section for collision between an ion and a molecule with a permanent dipole moment. An additional IM term accounting for the permanent dipole interaction is (ref. 6)

$$V_P = \frac{-\mu e \cos\theta}{R^2} \tag{3}$$

where μ is the dipole moment and θ is the angle between the negative half of the dipole and the R vector.

Theard and Hamill (ref. 6) included the V_P term with $\cos \theta = 1$ (for simplicity) and derived the following cross section contribution:

$$\sigma_D = \frac{\pi \mu e}{\epsilon} \tag{4}$$

They then explained the large cross sections observed for certain ion-polar molecule collisions in terms of a total σ given by $\sigma_D + \sigma_L$. These experimental results have been extended by Moran and Hamill (ref. 7). Their experiments have demonstrated that the ion-dipole term does make a large contribution to the observed cross section. The choice of equation (4) as the ion-dipole term presumes the dipole can always adjust to a maximum orientation in the ion field. This, however, is not generally the case. The ion transit time and rotational period would be expected to be important considerations.

The main purpose of this report is to present a preliminary description of a semiclassical treatment of ion-polar molecule capture collisions. It is intended that this approach be particularly useful to the experimenter. Throughout the study, the interaction is presumed to take place between an ion with velocity v_1 and a polar rotator which has no translational motion. The theoretical treatment is developed for both linear and symmetric top molecules and is comprised of the following three parts:

(1) Capture cross sections for low ion velocity are derived from quantum mechanical interaction potentials by simple averaging over rotational quantum numbers. In this region the ion field is effectively static and the IM interaction is treated as an "ion-induced" Stark effect. The manner in which various rotational distribution functions can be incorporated to calculate average cross sections is illustrated.

(2) Classically derived expressions for the capture cross section are presented for high ion velocity. This is a region of particular interest for the experimenter.

(3) Numerical results for the cross section are presented for hypothetical molecules of assigned dipole moments and electronic polarizabilities. These calculations are performed for randomized initial conditions at high ion velocity.

Finally, the numerical results are compared with both the low velocity predictions and the high velocity limiting values.

QUANTUM THEORETICAL CROSS SECTION AT LOW ION VELOCITY

Region of Theoretical Validity

Static field assumption. - The polar molecule Stark effect is defined as the splitting of rotational energy levels in a static electric field (ref. 8). In order for the ion field to

be considered effectively static, its rate of change must remain small compared to the molecular rotational frequency. This condition can be written (ref. 9) as

$$\frac{t_R}{F}\frac{dF}{dt} \ll 1 \tag{5}$$

In condition (5), F is the ion field ($= e/R^2$) and t_R is the rotational period of the polar molecule.

Condition (5) indicates the limit of validity for the low velocity treatment. The normalized rate of change of the radial component of the ion field is

$$\frac{1}{F_r}\frac{dF_r}{dt} = \frac{-2\dot{R}}{R} \tag{6}$$

If the ion velocity is approximately equal to the radial velocity, then condition (5) can be written as

$$\frac{2v_1}{R} t_R \ll 1 \tag{7}$$

At a rotational energy E_R of 0.05 electron volt, for a moment of inertia of $I = 10^{-40}$ gram-centimeter^2 (e.g., hydrochloric acid molecule, HCl), the rotational period is

$$t_R = 2\pi\left(\frac{I}{2E_R}\right)^{1/2} = 1.57\times10^{-13} \text{ sec} \tag{8}$$

If a 10-percent change in the ion field is allowed during the time t_R, the maximum ion velocity that satisfies condition (7) is

$$v_{max} = 3.18\times10^{11} R_c \tag{9}$$

where R_c is the distance of closest approach, which can be chosen as roughly equal to the impact parameter b_c. This is a lower limit choice for R_c, but the choice is not important since condition (5) is not the most restrictive condition for the validity of the treatment. For $R_c = 15$ angstroms, the maximum velocity from equation (9) is 4.8×10^4 centimeters per second. This value of R_c is estimated self-consistently by assuming $\pi R_c^2 = \sigma_D + \sigma_L$ for representative values of dipole moment and reduced mass. This ve-

locity corresponds to several times thermal energy for an IM pair with a relative mass of 50 atomic mass units. In general, condition (7) will not be fulfilled in the range of experimental ion energies; however, it will prove valuable to compare the trends of this theory with numerical results.

Perturbation approximation. - An additional restriction on the quantum mechanical approach arises from the Stark effect approximation. The derivations of the Stark interaction energies between ions and polar molecules are valid only if the field energy is a perturbation on the rotational motion (ref. 8). In fact, the ion-dipole interaction energy must be much smaller than the separations between rotational energy levels. This criterion can be written as

$$\frac{J\mu F}{E_R} << 1 \tag{10}$$

In this expression, J is the rotational quantum number and E_R is the rotational energy. The average energy level spacing is about E_R/J. For representative values, $J = 10$, $\mu = 1.5$ Debye units, and $E_R = 0.05$ electron volt, condition (10) with $J\mu F/E_R = 0.1$ is satisfied for an electric field F corresponding to $R = 67$ angstroms. This IM separation is several times the R_c employed previously. In fact, the ratio of the second to the first R_c value can be written as $(2M\mu e/h^2)^{1/4}$, which is always greater than unity. Thus condition (10), which specifies a minimum R, is more restrictive than equation (9).

Critical Impact Parameter

Gioumousis and Stevenson (ref. 4) have carried over Langevin's study of ion trajectories to calculate reaction cross sections. The interaction potential assumed is equation (1) but a critical reaction radius r_c is proposed for IM pairs. In reference 4 it is shown that ions which start toward the molecule at an impact parameter less than a critical impact parameter b_c will be captured. These captured ions will spiral inward until ion and molecule react inside a critical radius r_c. This quantity r_c should not be confused with the R_c of this report. The latter is the distance of closest approach for the impact parameter b_c. The critical impact parameter for the Langevin case is

$$b_c = \left(\frac{2\alpha_o e^2}{\epsilon}\right)^{1/4} = \sqrt{2}\, R_c \tag{11}$$

In this study the low velocity trajectories will be treated as in reference 4 for the

$C_1R^{-2} + C_2R^{-4}$ potential. An ion which approaches the polarizable polar molecule exactly at b_c will enter an unstable circular orbit of radius R_c. The derivation of the capture cross section from the assumed interaction potential will now be described.

Interaction Potential

Quantum mechanical expressions of the rotational Stark effects will be employed to obtain terms for the interaction potential. The quantum mechanical derivations of the first- and second-order Stark effects appear in reference 8. The total interaction potential is

$$V_{int} = \Delta W_1 + \Delta W_2 + V_L \tag{12}$$

where ΔW_1 and ΔW_2 are the first- and second-order Stark energies, respectively. The Langevin term V_L is included because polar molecules have polarizable distributions of electronic charge.

First-order Stark effect. - The interaction energy for the first-order Stark effect for the symmetric top molecule is (ref. 8)

$$\Delta W_{1T} = \frac{-\mu F M_J K}{J(J + 1)} \tag{13}$$

For the linear molecule, this effect is zero. Equation (13) gives the energy change in a static field for a symmetric top molecule such as methyl cyanide, CH_3CN. In equation (13), J is the total angular momentum quantum number, M_J denotes the component of J in the field direction, and K is the projection of J on the symmetry axis of the top. If the molecule can orient randomly relative to the field, then M_J ranges from +J to -J with equal probability. The quantum number K can also take on all values from +J to -J but not with equal probability. The relative probabilities of various K values depend on the molecular geometry and gas temperature (ref. 8). To predict these values one requires a relation between both J and K and the rotational energy.

The rotational energy of a symmetric top molecule is (ref. 10)

$$E_{RT} = \frac{J(J + 1)\hbar^2}{2I_B} + K^2\left(\frac{\hbar^2}{2I_A} - \frac{\hbar^2}{2I_B}\right) \tag{14}$$

In equation (14), I_B is the moment of inertia about an axis perpendicular to the symmetry

axis and I_A is the moment of inertia about the symmetry axis. Since (for constant temperature) the energy E_{RT} depends on J and K, once J is specified the values of K are governed by the molecular geometry. For a prolate top ("cigar like"), $I_A < I_B$, E_{RT} increases with K for constant J so that small K values are most probable. For an oblate top ("pancake like"), $I_B < I_A$, E_{RT} decreases with increasing K so that large values of K are most probable. The distribution of K values is further complicated by weighting factors that arise from nuclear spin statistics (ref. 8).

Classically, the first-order Stark effect is the orientation of a polar molecule such that it has a net dipole moment in the field direction. This occurs for a symmetric top molecule when the dipole moment has a component along the total angular momentum vector $\left(\mu K/\sqrt{J(J+1)}\right)$. The quantity M_J, equal to $\sqrt{J(J+1)}\cos\theta$, is the projection of J along the field and the projection of μ is $\mu M_J K/J(J+1)$.

For a linear polar molecule (e.g., HCl), the first-order Stark effect vanishes since $K = 0$ in equation (13). In this case there cannot be a component of μ parallel to J since $K/\sqrt{J(J+1)}$ is zero. This is strictly true only for diatomic molecules. It does not apply to linear polyatomic molecules which are excited to bending modes (ref. 8).

The rotational energy of a diatomic molecule is (ref. 11)

$$E_R = \frac{J(J+1)\hbar^2}{2I} \tag{15}$$

where I is the moment of inertia about an axis perpendicular to the internuclear (polar) axis.

Second-order Stark effect. - The second-order Stark interaction energy for the symmetric top molecule is (ref. 8)

$$\Delta W_{2T} = \frac{\mu^2 F^2 I_B}{\hbar^2}\left\{\frac{(J^2-K^2)\left(J^2-M_J^2\right)}{J^3(2J-1)(2J+1)} - \frac{\left[(J+1)^2-K^2\right]\left[(J+1)^2-M_J^2\right]}{(J+1)^3(2J+1)(2J+3)}\right\} \tag{16}$$

For the linear molecule, $K = 0$ and ΔW_2 becomes

$$\Delta W_{2R} = \frac{I_B \mu^2 F^2}{\hbar^2 J(J+1)}\left\{\frac{J(J+1) - 3M_J^2}{(2J-1)(2J+3)}\right\} \tag{17}$$

Classically, this effect corresponds to a nonuniform rotation of the molecule in the electric field. Under such conditions the dipole may spend most of the time lined up

either with or against the field. Thus the molecule will exhibit a net attraction or repulsion for the ion. Quantum mechanically, this corresponds to polarization of the wave function of a rigid rotator (ref. 8).

Capture Cross Section for a Linear Polar Molecule

Case of constant rotational energy. - The potential for the interaction between an ion and a linear polar molecule is

$$\left(V_{int}\right)_R = \Delta W_{2R} + V_L$$

$$= \frac{1}{2}\left[\frac{-2\mu^2 I}{\hbar^2 J(J+1)}\left\{\frac{J(J+1) - 3M_J^2}{(2J-1)(2J+3)}\right\}\right]\frac{e^2}{R^4} - \frac{\alpha_o e^2}{2R^4} \tag{18a}$$

Since the square of the electric field appears in ΔW_{2R}, the quantity in brackets can be interpreted as a rotational polarizability term α_{iR}. If then the total polarizability α_{tR} is defined as

$$\alpha_{tR} = \alpha_{iR} + \alpha_o \tag{18b}$$

equation (18a) can be written as

$$\alpha_{tR} = -\frac{2\left(V_{int}\right)_R}{F^2} \tag{18c}$$

Equation (18c) is analogous to the Langevin expression of equation (1). The partial cross section for a given M_J value can thus be written in the same form as the Langevin cross section. The electronic polarizability α_o is merely replaced by the total polarizability. Positive polarizabilities correspond to attractive interactions; repulsive collisions do not contribute to the capture cross section. The partial cross section is

$$\sigma_{tR} = \pi P_J\left[\frac{2\alpha_{tR}(M_J)e^2}{\epsilon}\right]^{1/2} \tag{19}$$

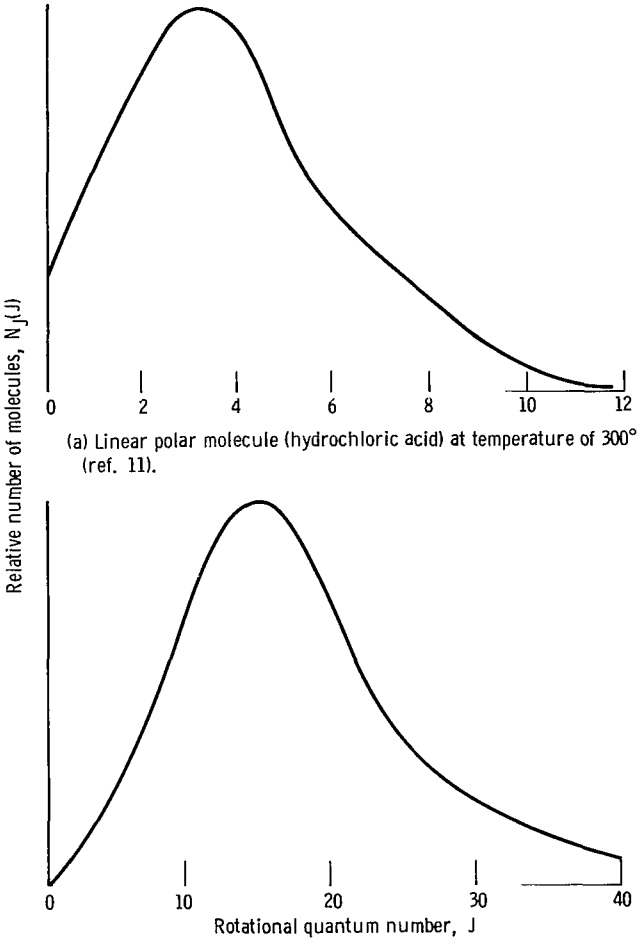

(a) Linear polar molecule (hydrochloric acid) at temperature of 300° K (ref. 11).

(b) Symmetric top polar molecule (methyl chloride) at temperature of 300° K (ref. 10).

Figure 1. - Distribution function among states of rotational quantum number J.

where P_J is the probability that the molecule is in the $\pm M_J^{th}$ state. The term α_{tR} is a function of M_J, the projection of J along the ion field. In equation (19), $\epsilon = Mv_1^2/2$ is the relative translational energy of the IM pair written in terms of the ion velocity v_1. The reduced mass M is $M_o M_1/(M_o + M_1)$ where M_o and M_1 are the molecule and ion masses, respectively.

Molecules with small moments of inertia will be in relatively low J states at normal gas temperatures. For example, the distribution of molecules in J states for HCl at 300° K is shown in figure 1(a) (ref. 11). For such "quantum rotators," the cross section must be calculated by summing all positive partial cross sections. Their values range from the first integral value of M_J which gives $+\alpha_{tR}$ up to J.

Molecules in high J states, that is "classical rotators," have distributions as shown in figure 1(b). For these molecules, the M_J states are effectively continuous and the summations over the positive polarizability values can be replaced by integrals. As shown in appendix B, in neither case does the cross section distinguish between positive or negative M_J. This is because the second-order Stark effect does not remove the M_J degeneracy (ref. 8).

The average cross section for zero electronic polarizability at high J taken from appendix B is

$$\bar{\sigma}_{iR} = \pi \left(\frac{\mu^2 e^2}{4E_R \epsilon} \right)^{1/2} \left[\sqrt{6} - \frac{\ln\left(\sqrt{3} + \sqrt{2}\right)}{\sqrt{6}} \right]$$

$$= \pi \left(\frac{\mu^2 e^2}{4E_R \epsilon} \right)^{1/2} (0.53) \cong \frac{\pi}{2} \left(\frac{\mu^2 e^2}{4E_R \epsilon} \right)^{1/2} \qquad (20)$$

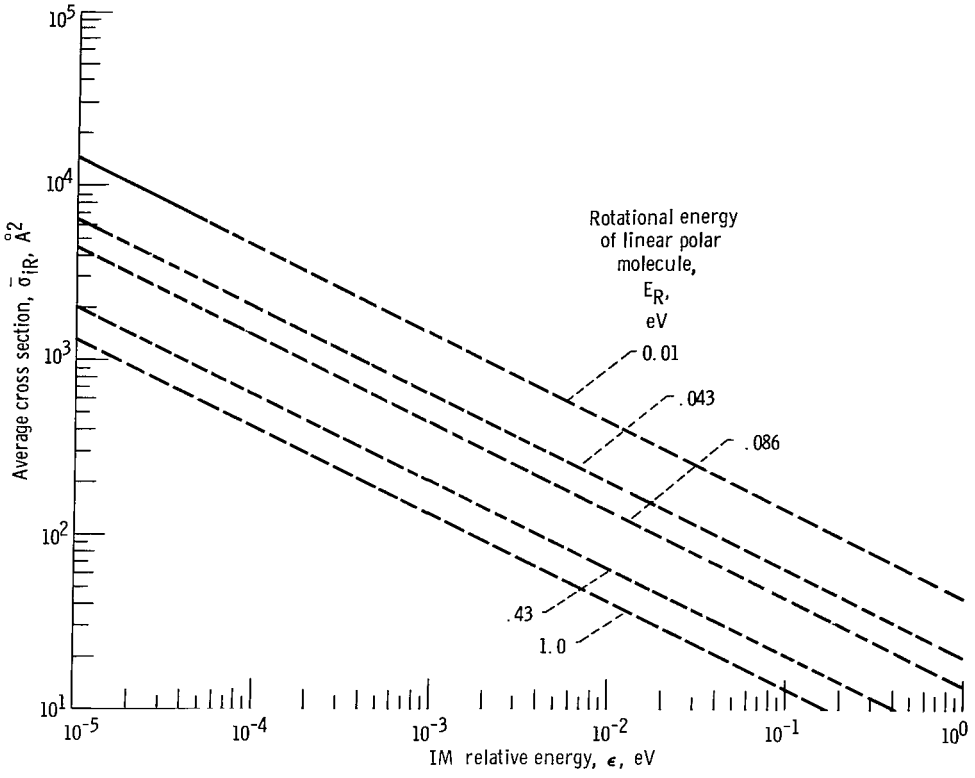

Figure 2. - Variation of average quantum mechanical cross section with relative ion-molecule energy for various molecular rotational energies. Linear polar molecule with zero electronic polarizability; dipole moment, μ = 1.67 Debye units; calculated from equation (20).

This cross section is plotted against ϵ in figure 2 for five different rotational energies and a constant value of μ ($\alpha_o = 0$). The upper limit to the region of exactness of the perturbation approximation is indicated by the solid curves. In all subsequent figures, dashed curves are used to indicate extensions beyond the ranges of validity.

The average cross section for nonzero electronic polarizability is where $\alpha_o \geq \mu^2/4E_R$ from appendix B:

$$\bar{\sigma}_{tR} = \pi \left(\frac{3\mu^2 e^2}{2E_R \epsilon}\right)^{1/2} \left[\frac{\sqrt{C+2}}{2\sqrt{3}} + \frac{C-1}{6} \ln\left(\frac{\sqrt{C+2}+\sqrt{3}}{\sqrt{C-1}}\right)\right] \tag{21}$$

where

$$C = \frac{4E_R \alpha_o}{\mu^2}$$

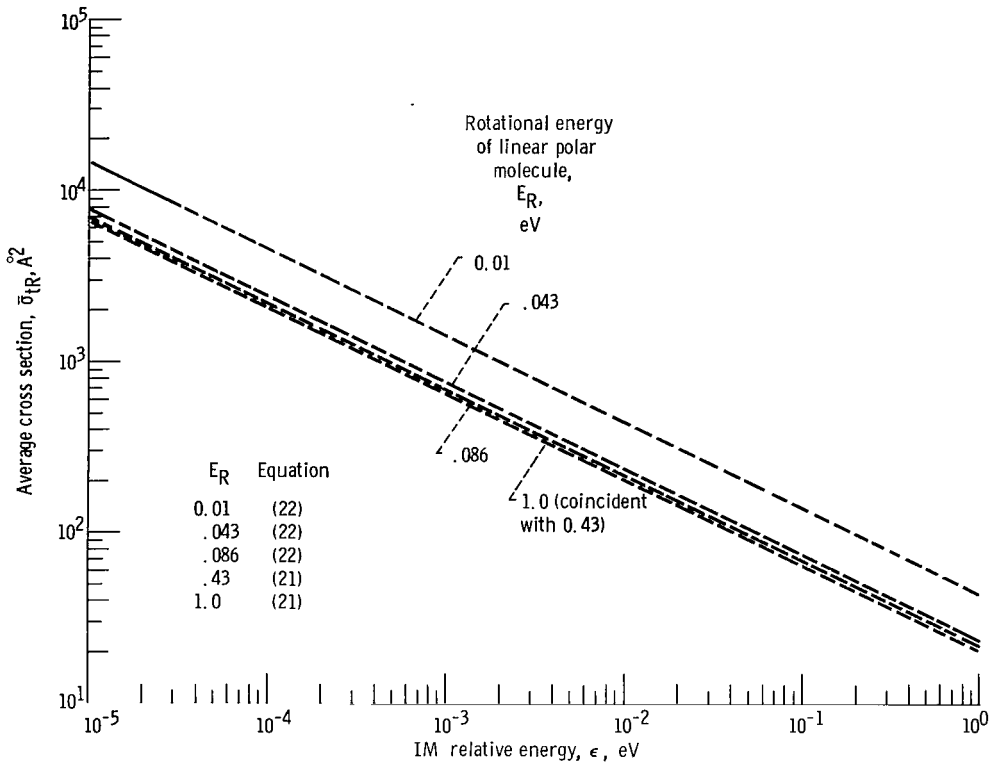

Figure 3. - Variation of average quantum mechanical cross section with relative ion-molecule energy for various molecular rotational energies. Linear polar molecule with nonzero electronic polarizability, α_0 = 1.67 angstroms^3; dipole moment, μ = 1.67 Debye units.

For $\alpha_o \leq \mu^2/4E_R$,

$$\bar{\sigma}_{tR} = \pi\left(\frac{3\mu^2e^2}{2E_R\epsilon}\right)^{1/2}\left[\frac{\sqrt{C+2}}{2\sqrt{3}} + \frac{C-1}{6}\ln\left(\frac{\sqrt{C+2}+\sqrt{3}}{\sqrt{1-C}}\right)\right] \tag{22}$$

The cross sections from equations (21) and (22) are plotted against ϵ in figure 3 for μ = 1.67 Debye units and α_o = 1.67 angstroms^3.

It must be emphasized that these average cross sections have been derived for fixed values of rotational energy (i.e., constant J). Such a procedure ignores the distribution of J values at the equilibrium gas temperature. These expressions do, however, prove valuable for comparison with numerical results even though the curves of figures 2 and 3 are extended considerably beyond the range of validity.

Rotational energy distribution function - linear molecule. - In equations (20) to (22) representative rotational energies were chosen that would be equal to kT for five values of temperature from 116^o to 11,600^{o}K. These values of E_R range from 0.01 to 1.0 electron volt.

In an experiment, however, the target molecules are actually distributed over a range of rotational energies as described by the distribution function f(J). This normalized function is (ref. 11)

$$f(J) = \frac{hB}{kT}(2J + 1)e^{-J(J+1)Bh/kT} \tag{23}$$

The average cross sections at a temperature T for constant ϵ are the normalized integrals of equations (20) to (22) weighted by f(J).

Capture Cross Section for Symmetric Top Polar Molecule

Case of constant rotational energy. - For the symmetric top, the first-order Stark term ΔW_{1T} (eq. (13)) must be included in the total interaction potential, in addition to the second-order Stark term ΔW_{2T} (from eq. (16)). The electrostatic interaction potential is then

$$\left(V_{int}\right)_T = \frac{-\mu e M_J K}{R^2 J(J + 1)} - \frac{\alpha_{tT} e^2}{2R^4} \tag{24}$$

where

$$\alpha_{tT} = -\frac{2\,\Delta W_{2T}}{F^2} + \alpha_o$$

is the total polarizability of the polar top. This quantity is the sum of the induced and electronic polarizability terms (R^{-4} terms). The partial cross section for capture can be derived by following an approach outlined in reference 5.

The effective potential for the ion-symmetric top interaction is

$$V_{eff} = \frac{L^2}{2MR^2} + \left(V_{int}\right)_T \tag{25}$$

In equation (25) the centripetal contribution $L^2/2MR^2$ is a fictitious potential term where L is the angular momentum ($Mv_1 b$). This term accounts for the relative motion of the IM pair, and its inclusion in this manner allows for a straightforward cross section

derivation. In conventional notation, the first-order interaction term ΔW_{1T} may be written as $-\mu_{12}e/R^2$ where μ_{12} is the dipole moment matrix element (ref. 8). Let the effective angular momentum term be

$$L_{eff}^2 = L^2 - 2\mu_{12}eM = (Mv_1b)^2 - 2\mu_{12}eM \tag{26}$$

The maximum of the effective potential is at the critical distance of closest approach on the crest of the angular momentum barrier. Since

$$\left(\frac{\partial V_{eff}}{\partial R}\right)_{R=R_c} = 0 \tag{27a}$$

then

$$\frac{L_{eff}^2}{2MR_c^2} = \frac{\alpha_{tT}e^2}{R_c^4} \tag{27b}$$

From equation (27b), the expression for the distance of closest approach is

$$R_c^2 = \frac{2M\alpha_{tT}e^2}{L_{eff}^2} \tag{28}$$

The translational energy at infinite distance is equal to the effective potential at R_c. This is true if the rotational energy of the molecule is effectively constant. This condition can be written as

$$\epsilon = \left(\frac{1}{2}Mv_1^2\right)_{R=\infty} = \left(V_{eff}\right)_{R=R_c} \tag{29}$$

However, $\left(V_{eff}\right)_{R=R_c}$ is simply $1/2\left(L_{eff}^2/2MR_c^2\right)$ because

$$V_{eff} = \frac{L_{eff}^2}{2MR_c^2} - \frac{\alpha_{tT}e^2}{2R_c^4} = \frac{L_{eff}^2}{2MR_c^2} - \frac{1}{2}\left(\frac{L_{eff}^2}{2MR_c^2}\right) \tag{30}$$

The final form of equation (30) is obtained by substitution for $\alpha_{tT}e^2/R_c^4$ from equation (27b).

Substituting the expression for R_c^2 from equation (28) into equation (30) gives the following relation for ϵ:

$$\epsilon = \frac{L_{eff}^4}{8M^2\alpha_{tT}e^2} = \frac{\left[(Mv_1b_c)^2 - 2\mu_{12}eM\right]^2}{8M^2\alpha_{tT}e^2} \tag{31}$$

In equation (31), b_c is the critical impact parameter corresponding to the distance of closest approach R_c. Rearranging and taking the square root of both sides of equation (31) give

$$(Mv_1b_c)^2 - 2\mu_{12}eM = \left(8M^2\alpha_{tT}e^2\epsilon\right)^{1/2} \tag{32}$$

If equation (29) is used for $Mv_1^2/2$, the partial cross section for the ion-symmetric top capture collision is

$$\sigma_{tT} = \pi b_c^2 = \pi\left[\frac{\mu_{12}e}{\epsilon} + \left(\frac{2\alpha_{tT}e^2}{\epsilon}\right)^{1/2}\right] \tag{33}$$

In equation (33) both terms are functions of M_J and K.

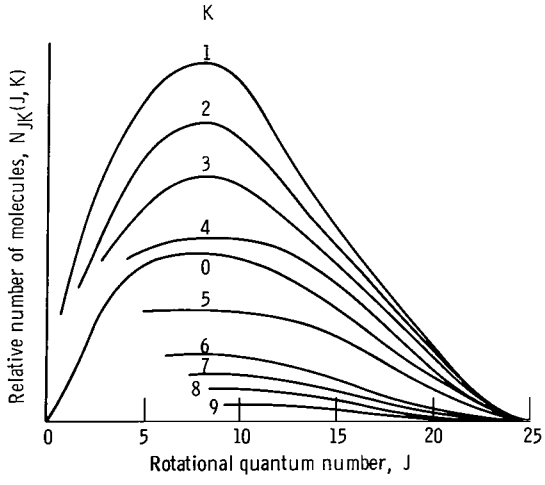

Figure 4. - Distribution function among states of rotational quantum number J for a symmetric top polar molecule for various quantum numbers, K, and $I_B = 5I_A$ (ref. 10).

The partial cross sections for the symmetric top cannot be simply averaged over the quantum numbers M_J and K. Although all values of M_J are equally probable, the values of K for constant J obey a distribution function $f_J(K)$. However, it is more conventional to consider the distribution function $f_K(J)$ for constant K.

Distributions $f_K(J)$ for the parameter K are shown in figure 4 for a sample symmetric top. For this molecule it is assumed that all nuclei have very large spins. Levels for which K is a multiple of three must be doubly weighted for particles of spin 1/2 which rotate about the symmetry axis. The K value assignment to be

made in the next paragraph was consistent with the initial conditions of the numerical study.

The partial cross section for the ion-symmetric top capture collision at high J for a fixed K is obtained by substituting for μ_{12} and α_{tT} in equation (33). This partial cross section is

$$\sigma_{tT} = \pm \frac{\pi \mu e}{2\sqrt{2} J \epsilon} M_J + \frac{\pi}{4J} \left(\frac{19 \mu^2 e^2}{E_R \epsilon} \right)^{1/2} \left\{ \frac{\left[J^2 \left(\frac{16 E_R}{\epsilon_c} - 5 \right) + M_J^2 \right]^{1/2}}{19} \right\} \tag{34a}$$

In equation (34a) the value of $K = \pm J/2\sqrt{2}$ is assigned by solving equation (14) with $I_B = 5I_A$. This moment of inertia ratio was used in the numerical study.

The average cross section is

$$\bar{\sigma}_{tT} = \left[\frac{\pi \mu e}{2\sqrt{2} J^2 \epsilon} \int_{(M_J)_{min}}^{(M_J)_{max}} M_J \, dM_J + \frac{\pi}{4J^2} \left(\frac{19 \mu^2 e^2}{E_R \epsilon} \right)^{1/2} \int_{(M_J)_{min}}^{(M_J)_{max}} \left(M_J^2 \pm a^2 \right)^{1/2} dM_J \right] \tag{34b}$$

In equation (34b)

$$a^2 = \frac{\frac{16 E_R}{\epsilon_c} - 5}{19}$$

and the probability that the top is in the $+M_J^{th}$ state $P'_J = (1/2J)$ has been included. Equation (34b) integrates to

$$\bar{\sigma}_{tT} = \frac{\pi \mu e}{4\sqrt{2} \epsilon J^2} \left(M_{max}^2 - M_{min}^2 \right) + \frac{\pi}{8J^2} \left(\frac{19 \mu^2 e^2}{E_R \epsilon} \right)^{1/2} \left\{ M_J \left(M_J^2 \pm a^2 \right)^{1/2} \pm a^2 \ln \left[M_J + \left(M_J^2 \pm a^2 \right)^{1/2} \right] \right\} \Bigg|_{(M_J)_{min}}^{(M_J)_{max}} \tag{34c}$$

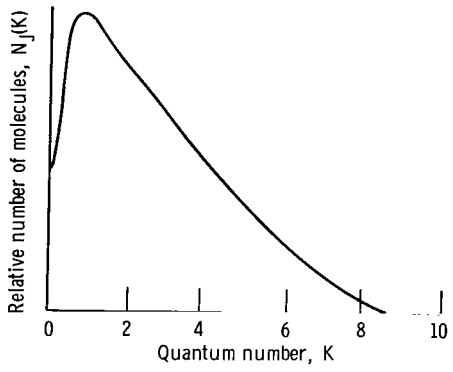

Figure 5. - Distribution function among states of quantum number K for symmetric top polar molecule from figure 4 for rotational quantum number J of 9.

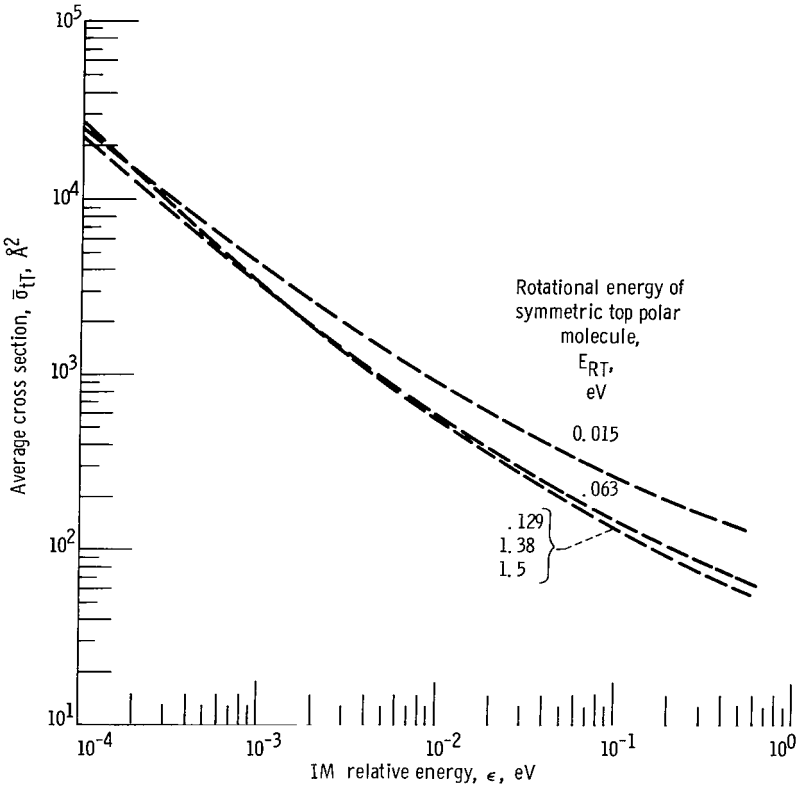

Figure 6. - Variation of average quantum mechanical cross section with relative ion-molecule energy for various molecular rotational energies. Symmetric top polar molecule with nonzero electronic polarizability, α_0 = 1.67 angstroms^3; dipole moment, μ = 1.67 Debye units; calculated from equation (34c).

The limits of integration in equation (34c) are defined by the condition that the integrand of equation (34a) be positive.

The rotational energy is again held constant and corresponds to a representative molecule with $E_{RT} = (3/2)kT$. For simplification it is assumed that the initial K value is specified by equipartition of energy and is $\pm J/2\sqrt{2}$. Actually the distribution $f_J(K)$ for constant E_{RT} depends on the molecular geometry and temperature. A sample of the function $f_J(K)$ for a top with $I_B = 5I_A$ is shown in figure 5. The average cross section for fixed rotational energy and nonzero electronic polarizability is plotted in figure 6.

Rotational energy distribution function - symmetric top. - The average cross section for constant J and a fixed K value is not directly usable by the experimentalist. Rather, the average over the total distribution function f(J, K) is the experimental quantity of interest. This normalized distribution function is (ref. 8)

$$f(J, K) = \left[\frac{B^2Ah^3}{\pi(kT)^3}\right]^{1/2} (2J + 1)e^{-[J(J+1)B+K^2(A-B)]\hbar^2/kT}$$

where $A = h/8\pi^2 I_A$. As mentioned earlier, the moment of inertia I_A will be greater than I_B for an oblate top and less than I_B for a prolate top. For a constant temperature the lower values of K are more probable for a prolate top. The higher values of K become more probable for an oblate top.

The average cross sections at a given ϵ which are of interest to the experimentalist are

$$\bar{\sigma}(\epsilon) = \int_J \int_K \bar{\sigma}(J, K) f(J, K) dJ\, dK \tag{35}$$

The cross section $\bar{\sigma}(J, K)$ must be previously integrated over a random distribution of M_J values.

CLASSICAL CROSS SECTIONS AT HIGH ION VELOCITY

Two Limiting Cross Section Expressions

In the region of high ion velocity, two classical expressions can be obtained for the capture cross section for extreme conditions of collision behavior. The first is a rigorous upper limit to the capture cross section obtained from the condition that the dipole can always orient so as to attract the ion. The second is an approximate cross section

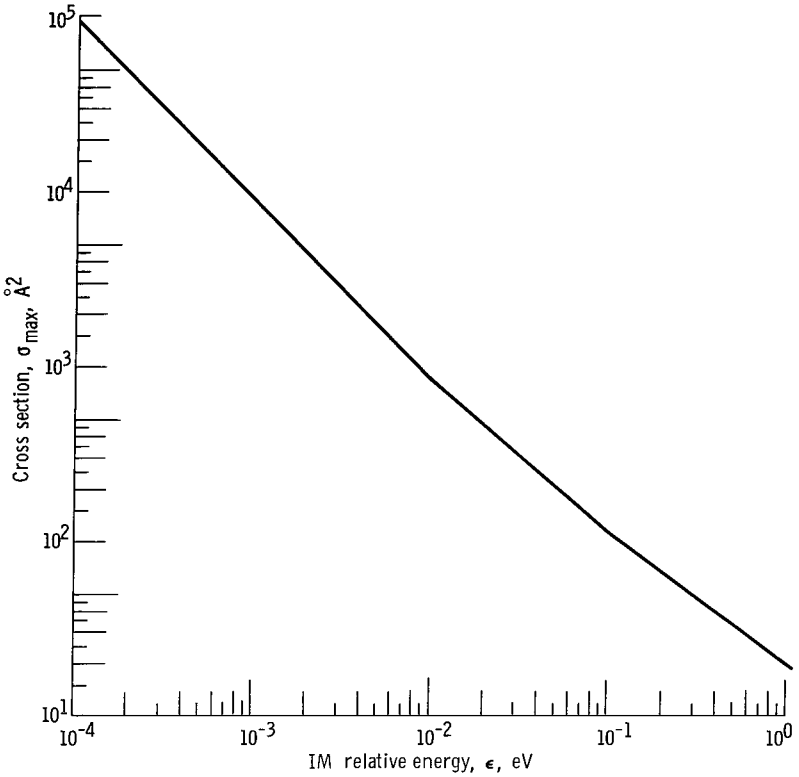

Figure 7. - Variation of classical maximum cross section with relative ion-molecule energy. Nonzero electronic polarizability, α_0 = 1.67 angstroms^3; dipole moment, μ = 1.67 Debye units; calculated from equation (36).

obtained from the condition that the collision time is much shorter than the rotational period. The latter expression is not rigorous but is conceptually useful in discussing collision behavior in this regime.

Upper limit cross section. - As explained earlier, the maximum cross section for an ion-polar molecule collision independent of molecular geometry is

$$\sigma_{max} = \frac{\pi \mu e}{\epsilon} + \sigma_L \tag{36}$$

This is precisely the expression used in references 6 and 7 to fit experimental IM data. It says that regardless of the ion trajectory the dipole can always orient favorably for capture. This is a type of adiabatic approximation where it is assumed that the Hamiltonian changes very slowly. This rate of change must be sufficiently slow so that the dynamical system can always act to minimize the energy. Such an approach clearly ignores the rotational energy of the target molecules. This assumption actually violates conservation of energy since it takes no account of rotational acceleration or deceleration accompanying collision. This cross section is plotted in figure 7.

Estimated capture cross section. - The condition for the static orientation approximation is that the IM interaction time be very much shorter than the period of molecular rotation (ref. 12). This condition can be written as

$$\frac{t_R}{t_c} >> 1 \tag{37}$$

where t_c is the collision time and t_R is given by equation (8). The quantity t_c can best be written in terms of the relative velocity and a characteristic interaction distance R_h. A meaningful choice for R_h is the distance at which the rotator can first be completely "hindered" by a static ion field, that is, cannot make a complete rotation. Then R_h is defined by

$$R_h = \left(\frac{\mu e}{E_R}\right)^{1/2} \tag{38}$$

The quantity t_c becomes

$$t_c = \frac{R_h}{v_1} = \left(\frac{\mu e}{E_R}\right)^{1/2} \frac{1}{v_1} \tag{39}$$

For a molecule with $E_R = 0.05$ electron volt $= 8\times10^{-14}$ erg, the interaction distance for a dipole moment of 1.67 Debye units is 10 angstroms. The minimum velocity at which the sudden approximation is valid, for $t_R/t_c = 10$ and t_R given by equation (8), is

$$v_{min} = \frac{10^{-1} R_h}{t_R} = \frac{10^{-8}}{1.57\times10^{-13}} \text{ cm sec}^{-1} \cong 6\times10^6 \text{ cm sec}^{-1} \tag{40}$$

Letting $\mu_{12} = \mu \cos\theta$ and $\alpha_{tT} = \alpha_o$ in equation (33) yields the partial cross section

$$\sigma_\theta \equiv \pi b_c^2 = \frac{\pi\mu e}{\epsilon} \cos\theta + \sigma_L \tag{41}$$

Equation (41) is written with the assumption that the form of equation (33) is valid both for the high and low interaction energies (velocities). Equation (41) means that all ions which approach at less than the critical impact parameter b_c will be captured.

It can be argued that some ions which are initially attracted as specified by equation (41) will enter orbits that later become repulsive. This effect could occur as the ion spirals inward but before the R value becomes less than the r_c of reference 4. (The numerical results indicate only a small fraction of collisions behave this way.) The averaging procedure which will be described does, however, provide an instructive limiting case.

The average cross section is simply the normalized integral over the partial cross sections independent of rotational energy. It is assumed that the dipole has no time to adjust in the ion field. The differential solid angle is $d\Omega = \sin\theta\, d\theta\, d\varphi$. The static orientation average cross section is

$$\bar{\sigma}_\theta = \frac{1}{2}\,\frac{\pi\mu e}{\epsilon}\int_0^{\theta_{max}} \cos\theta \sin\theta\, d\theta + \frac{\pi}{2}\left(\frac{2\alpha_o e^2}{\epsilon}\right)^{1/2}\int_0^{\theta_{max}} \sin\theta\, d\theta \tag{42a}$$

The factor of 1/2 in equation (42a) comes from the $\int_0^{2\pi} d\varphi$ divided by the solid angle normalization factor 4π. The value of θ_{max} is determined from the condition that equation (41) be positive. In terms of $\cos\theta$ this occurs when

$$(\cos\theta)_{min} = -\left(\frac{2\alpha_o\epsilon}{\mu^2}\right)^{1/2} = -\left(\frac{\epsilon}{\epsilon_c}\right)^{1/2} \tag{42b}$$

where the critical energy ϵ_c is $\left(\mu^2/2\alpha_o\right)$.

Equation (42a) can be written as

$$\bar{\sigma}_\theta = \frac{\pi\mu e}{2\epsilon}\int_{(\cos\theta)_{min}}^{1} \cos\theta\, d(\cos\theta) + \frac{\pi}{2}\left(\frac{2\alpha_o e^2}{\epsilon}\right)^{1/2}\int_{(\cos\theta)_{min}}^{1} d(\cos\theta) \tag{43}$$

Upon integration, and substitution of the expression for $(\cos\theta)_{min}$, equation (43) becomes

$$\bar{\sigma}_\theta = \frac{\pi\mu e}{4\epsilon}\left(1 - \frac{\epsilon}{\epsilon_c}\right) + \pi\left[\left(\frac{\alpha_o e^2}{2\epsilon}\right)^{1/2} + \frac{\alpha_o e}{\mu}\right] \tag{44}$$

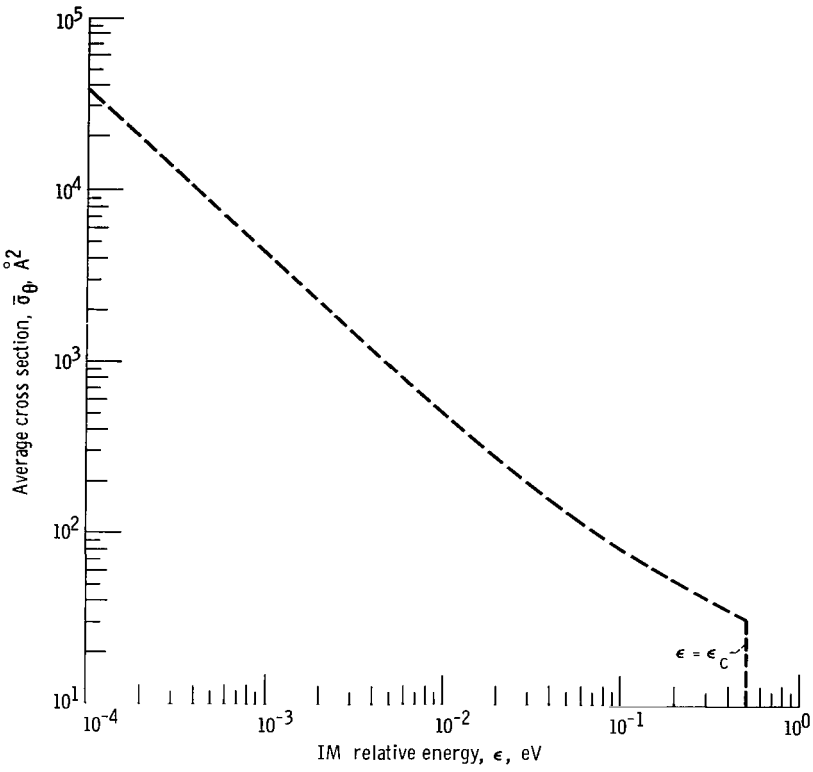

Figure 8. - Variation of average static orientation cross section with relative ion-molecule energy. Nonzero electronic polarizability, α_0 = 1.67 angstroms^3; dipole moment, μ = 1.67 Debye units; calculated from equation (44).

This cross section of equation (44) reduces to $\sigma_L = \pi\left(2\alpha_o e^2/\epsilon\right)^{1/2}$ at the critical energy ϵ_c. It is plotted against ϵ in figure 8 for μ = 1.67 Debye units and α_o = 1.67 angstroms^3 independent of rotational energy. Condition (37) is, of course, the lower limit to the region of validity of this sudden approximation. From equation (40) for an E_R value of 0.05 electron volt and M = 50 atomic mass units, the minimum value of ϵ is 1000 electron volts. This minimum energy is three orders of magnitude greater than the largest value of the abscissa in figure 8.

Numerical Treatment

Need for a numerical high velocity treatment. - Quantum rotators have energy level separations which are significant compared to kT and cannot be considered continuous. However, the IM interaction potential at high ion velocity cannot be considered a perturbation on the rotational motion. In fact, neither J, K, nor M_J are good quantum numbers when critical impact parameters are of the order of molecular diameters. The complete approach to a collision theory in this regime, therefore, must be by means of

a quantum mechanical treatment. Such a description would require an exact calculation of a time-dependent strong field Stark effect. That problem is clearly intractable and its consideration is beyond the scope of this report. On the other hand, classical rotators with J about 10 or greater have energy levels that can be regarded as continuous. Most molecules with I values greater than 10^{-40} gram-centimeter^2 will be excited to these J values at normal temperatures. From this viewpoint the high velocity IM interaction can be considered purely classical. However, both the direction and magnitude of the rotational angular momentum will vary during interaction and these effects should also be considered. To treat this classical collision satisfactorily it is necessary to solve the equations of motion numerically for the entire IM system. This method of attack will be outlined in the next section and results will be presented for hypothetical molecules.

Models and general approach. - The ion-dipole interaction in the classical limit was studied by numerical solution of the equations of motion for two different models, which are approximations to real molecular systems. The target for model I was a rigid rotator polar molecule with a permanent dipole moment along the internuclear axis. This polar molecule was allowed to interact with an ion moving translationally relative to its center of mass. The target for model II consisted of a rigid symmetric top molecule with a dipole "frozen" in it along the symmetry axis. The ion was treated just as in model I.

Coupled differential equations were written for the two physical models, and the models were programed in Fortran IV for solution on the IBM 7094 digital computer. The Lagrangian formulation of the force equations was utilized for each model. The conservation of energy equation was carried along to check the accuracy of the integration technique.

The coordinate system used for model I appears in figure 9. A discussion of this system is included in appendix C. The values of the constants chosen for the linear molecule and a discussion of the translational energy approximation appear in appendix D; also included in appendix D is a discussion of the assignment of initial conditions to the variables and their time derivatives.

A total of 36 cases was solved for constant (initial) rotational energy for each impact parameter. The orientations of the negative end of the dipole and plane of rotation were varied relative to the ion path. This was done to completely randomize the initial conditions on the IM pair with the ion effectively at infinity.

The IM interaction potential is composed of both the ion-dipole and polarization terms. The polarization term is simply $-\alpha_o e^2/2R^4$. However, the ion-dipole term is a complicated expression containing four different angles. The IM total energy expression and derivation of the equations of motion are also included in appendix E.

The numerical study of the symmetric top target molecule was performed to investigate the effect of molecular geometry on the time-dependent IM interaction. The coordi-

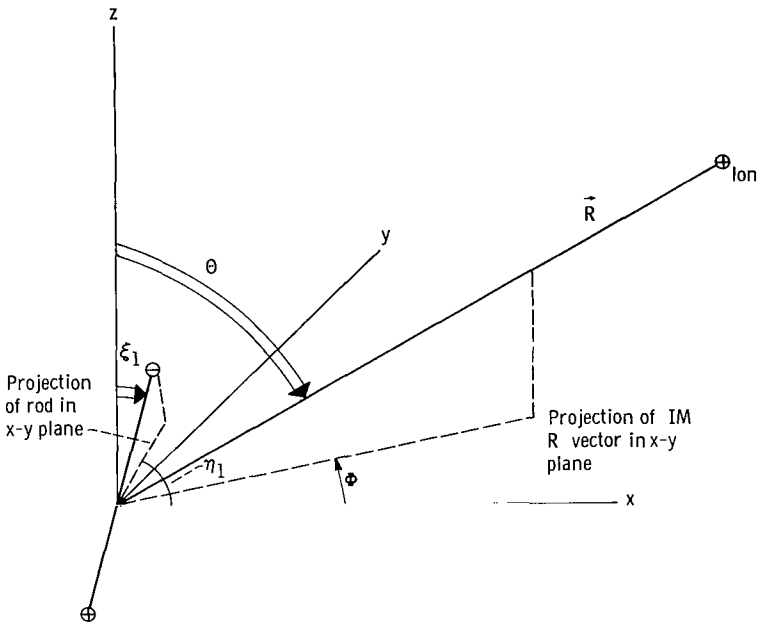

Figure 9. - Coordinate system employed in the computer study of interaction between an ion and a linear polar molecule.

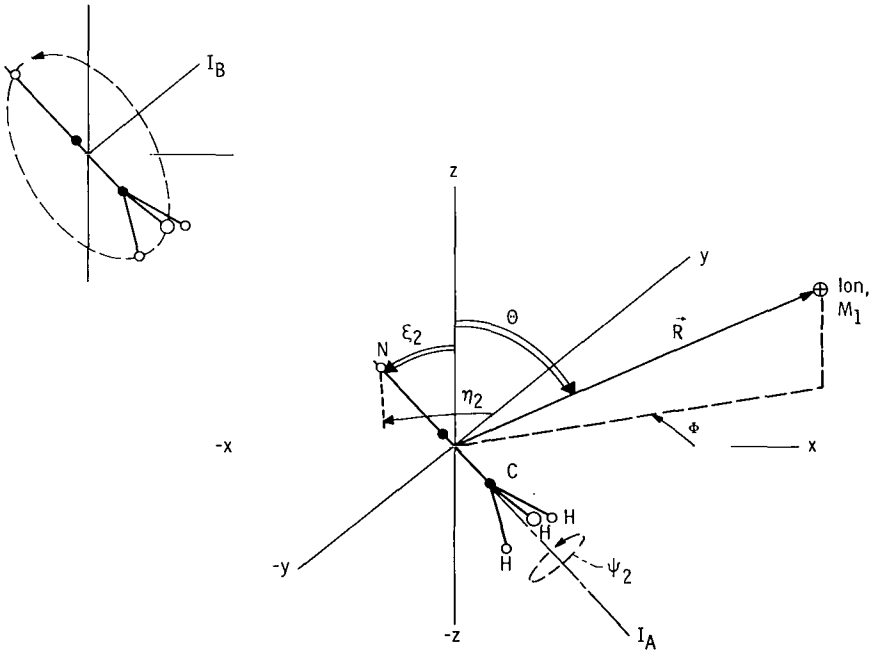

Figure 10. - Coordinate system employed in computer study of interaction between an ion and a symmetric top polar molecule.

nate system used to describe the ion-symmetric top interaction is shown in figure 10. The randomization of initial conditions was performed similar to model I. Additional considerations regarding the extra degree of rotational freedom are discussed in appendix F. The derivation of the equations of motion is also included therein.

Definition of the numerically calculated cross section. - The numerically calculated capture cross section is

$$\sigma_{ci} \equiv \pi b_{ci}^2 \tag{45}$$

where $i = 1$ or 2 identifies the molecular model. The critical impact parameter b_{ci} which defines the capture cross section is not a conventional impact parameter like b_c. The latter is the value of b below which capture collisions occur with unit probability. However, although the $-\alpha_o e^2/2R^4$ potential is always attractive, the $-\mu e/R^2 \cos\theta$ term has a repulsive phase. Since the ion permanent dipole potential can thus prevent capture of ions, b_{ci} is best defined in terms of a collision ratio C_R. The quantity C_R is the fraction of IM cases tried which result in collision for an assigned impact parameter b. The capture cross section is then defined by

$$\sigma_{ci} = \int C_R(b)\, dA_c \tag{46}$$

The quantity dA_c in the differential collision area or cross section $d(\pi b^2) = 2\pi b\, db$. Equation (46) can then be rewritten as

$$\sigma_{ci} = \pi \int_0^{b_0^2} C_R(b)\, d(b^2) \tag{47}$$

where b_0 is the largest value of b for which any collisions are observed. The square of the critical impact parameter for capture is simply

$$b_{ci}^2 = \int_0^{b_0^2} C_R(b)\, d(b^2) \tag{48}$$

Normalization is insured since $\int b\, db = b^2/2$ and the 2 cancels the 2 from $d(b^2)$. The square of the critical impact parameter for capture is obtained directly by measurement of the area under the curve C_R against b^2.

RESULTS AND DISCUSSION

Qualifications Regarding the Quantum Theoretical Cross Section

For the hypothetical molecule examined numerically, $I = 3.85 \times 10^{-38}$ gram-centimeter^2 and the IM interaction cannot be considered a perturbation for velocities greater than 10^3 centimeters per second. This value of v_1 corresponds to an IM energy of about 10^{-5} electron volt for a representative value of reduced mass. This velocity is 1/50 of the minimum value assigned in the numerical calculation. In the regime of velocities included in the computer study, transitions between rotational states do not obey quantum mechanical selection rules; rather, the rotational energy varies through a continuum of states under the influence of the ion field. This field is time dependent and a quantum mechanical description of the IM interaction is an intractable problem. However, it does prove useful to assume that the continuum average of the matrix elements approximates the classical time-averaged behavior. There is no guarantee that this situation will hold true in the region where numerical results are to be compared with theoretical predictions. Nevertheless, the average quantum mechanical expressions do provide a convenient framework for qualitative discussion of numerical results.

It is also true that the quantum mechanical cross sections were derived for constant J. It is obvious that J and M_J will vary during a representative interaction. In the derivation of the quantum mechanical expressions it was assumed that all values of M_J remain equally probable for a fixed J. This approximation is equivalent to assuming that M_J varies randomly during an average collision.

Numerical Results for Model I

Curves of C_R against b^2 for $E_R = 0.043$ and 0.086 electron volt are shown in figures 11(a) and (b). These plots are for ion velocities of 5.5×10^4 and 10^5 centimeters per second, respectively. These velocities correspond to IM relative energies of 0.05 and 0.16 electron volt for an M value of 32 atomic mass units. The shape of such plots is sensitive to values of both rotational energy and ion velocity. The error in calculating the numerical cross section is roughly b_{ci}^2/n, where n denotes the number of cases attempted for random initial orientations at a given b value.

Computer checks of the orientation of the rotational plane indicate that it is effectively random for a representative collision. This gives credibility to the assumption that all M_J values were given equal probability in the derivations of the quantum mechanical cross sections. The cross section values σ_{c1} against ϵ are shown for the two rotational energies together with the quantum mechanical curves in figure 12. On

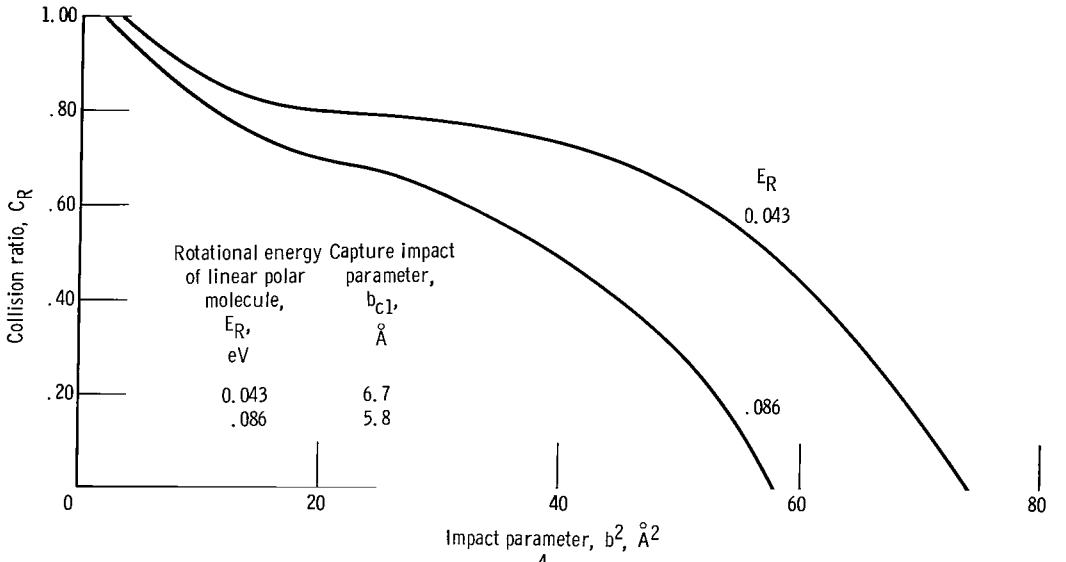

(a) Ion velocity, 5.5×10^4 centimeters per second.

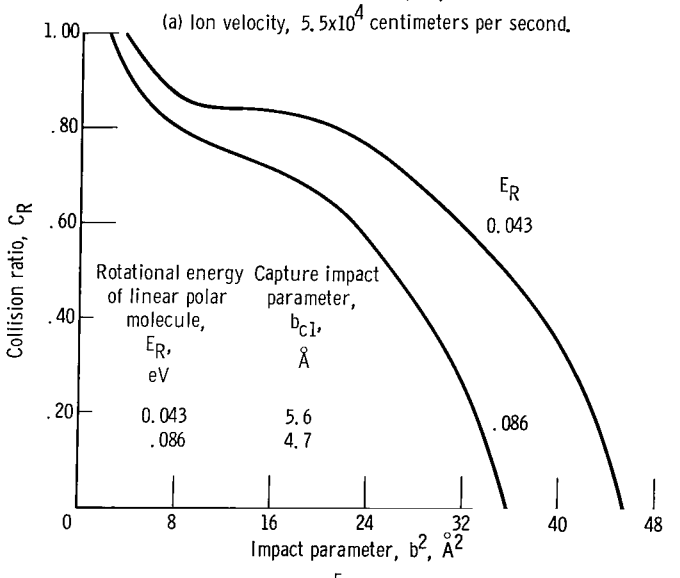

(b) Ion velocity, 10^5 centimeters per second.

Figure 11. - Variation of collision ratio with free particle impact parameter for two different rotational energies. Nonzero electronic polarizability, $\alpha_0 = 1.67$ angstroms^3; dipole moment, $\mu = 1.67$ Debye units.

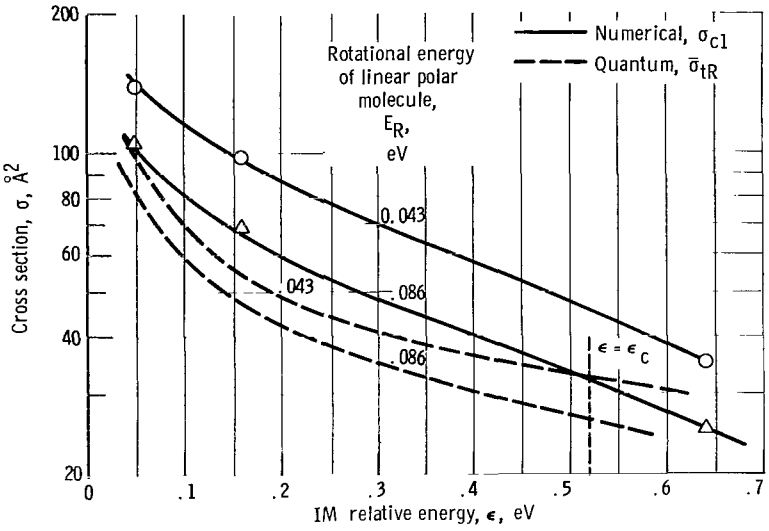

Figure 12. - Comparison of numerically calculated cross section σ_{c1} and average quantum mechanical cross section $\bar{\sigma}_{tR}$ for linear molecule. Nonzero electronic polarizability, α_0 = 1.67 angstroms^3; dipole moment, μ = 1.67 Debye units.

the simple comparison basis which has been adopted, the fact that the σ_{c1} values are 20 to 80 percent larger than the quantum theoretical values can be accounted for by the net lowering of the initial E_R value during collision. Monitoring of the machine problem was done with an additional subroutine. Results from this check indicate that the rotor is usually decelerated when the ion reaches its turning point. The average value of J calculated in the numerical study can then be interpreted as an indication of the degree to which the rotation is polarized by the field. Classically, this effect corresponds to nonuniform motion of the dipole in the ion field. Once the ion reaches the hindering distance R_h the field tends to line up the dipole but is allowed only a limited time to do so. The dependence of σ_{c1} on rotational energy is very nearly the $E_R^{-1/2}$ dependence which is predicted for $\bar{\sigma}_{tR}$.

Comparison is made between the σ_{c1} values and predictions of σ_{max} (eq. (36)) and $\bar{\sigma}_\theta$ (eq. (44)) in figure 13. Below ϵ = 0.10 electron volt, the numerical cross section shows a more gradual dependence on ϵ than the σ_{max} curve. The curve of $\bar{\sigma}_\theta$ as a function of ϵ is somewhat different from the plots of σ_{c1} as a function of ϵ.

Comparison between σ_{c1} and the Langevin cross section from equation (1) is made in figure 14. Both σ_{c1} plots give considerably larger cross sections than σ_L throughout the range of ϵ. It is evident that reaction cross sections measured for linear polar molecules are mainly the result of the ion-permanent dipole interaction. This situation will hold true unless μ is very small (e.g., the carbon monoxide molecule, CO). Although the Lagrangian contains the sum of two potential terms, their average contribution to the capture cross section is not simply the maximum $\sigma_D + \sigma_L$. Meaningful experimental cross sections can be obtained by integrating the numerical results over the distribu-

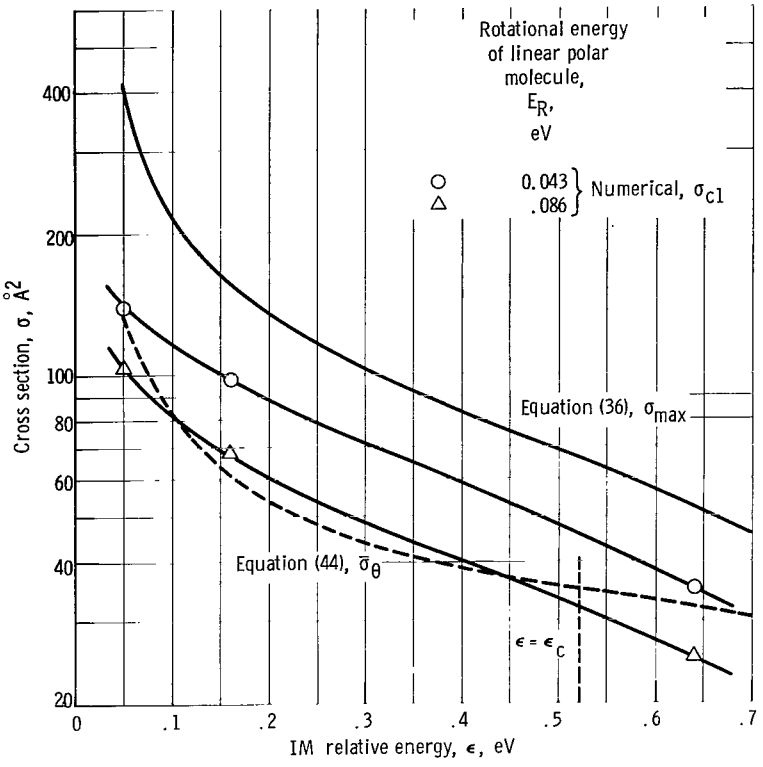

Figure 13. - Comparison of numerically calculated cross section σ_{cl} for linear molecule with two classical cross sections σ_{max} and $\bar{\sigma}_\theta$.

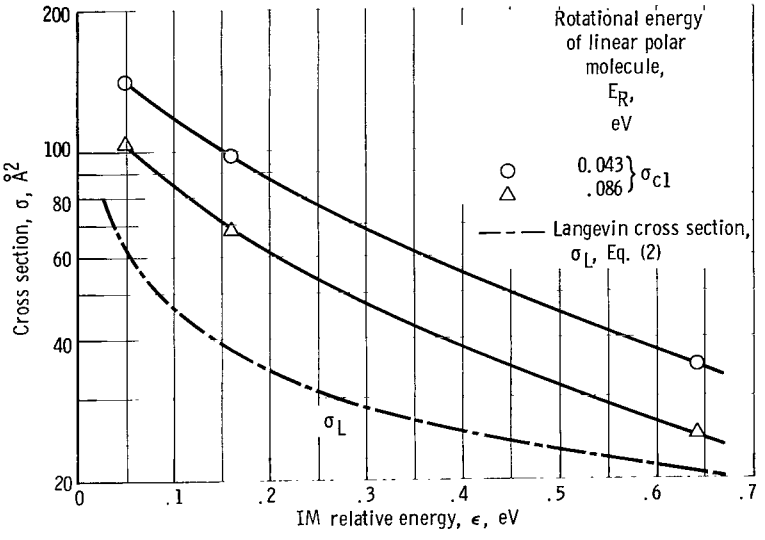

Figure 14. - Comparison of numerically calculated cross section σ_{cl} for linear molecule and Langevin cross section σ_L.

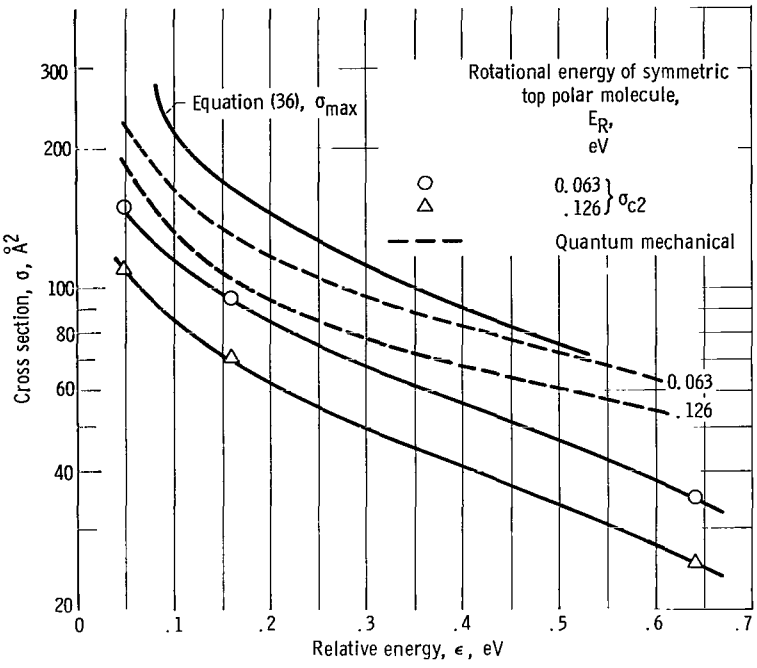

Figure 15. - Comparison of numerically calculated cross sections and average quantum mechanical cross section for symmetric top molecule.

tion function in rotational energy.

Numerical Results for Model II

The numerical results for the ion-symmetric top capture cross section are shown in figure 15. This capture cross section displays the same dependences on rotational and translational energy as the linear molecule cross section.

The average quantum mechanical cross sections are also plotted in figure 15 for E_{RT} = 0.063 and 0.123 electron volt. The main contribution to the quantum theoretical cross section, equation (34b), is from the polarizability term. This behavior is consistent with the fact that the numerically calculated symmetric top cross sections are only slightly larger than the corresponding linear molecule values of figures 12 to 14. These results indicate that the additional degree of rotational freedom for the symmetric top has little effect on the capture cross section for this hypothetical molecule. Classically, this corresponds to a negligible first-order Stark contribution to the capture cross section. The values of the numerically calculated cross sections are smaller than the average quantum mechanical values throughout the range of ϵ. This is in contrast to the behavior of the ion-linear molecule capture cross section.

Since the component of angular momentum along the symmetry axis will vary during

interaction, the ion-symmetric top collision has an additional complication. Not only J and M_J but also K will take on values different from the initial value as the ion approaches the molecule. Any detailed discussion of the similarity between the two sets of numerical results must await further numerical checks and interpretation.

Comparison of Experimental and Numerical Results

As shown in figures 13 and 15, the numerical capture cross sections for the hypothetical molecules are smaller than the maximum IM capture cross section of equation (36), especially at low values of ϵ. The latter expression has been used to fit data from experiments done at gas temperatures of 500° K (refs. 6 and 7). The numerical results also indicate the capture cross section has a gradual dependence on IM relative energy that is less than $\epsilon^{-1/2}$. This should be contrasted with the ϵ^{-1} dependence which has been reported for certain IM reaction cross sections (refs. 6 and 7). This disparity may suggest that the role of spurious effects accompanying low electric field experiments should be investigated. Other experimenters have reported difficulty in specifying the ion energy and trajectory at low electric fields (ref. 13).

CONCLUDING REMARKS

Up to the present, experimental studies of IM capture cross sections have ignored the effect of rotational energy of the target molecule. However, the present numerical treatment indicates that the capture cross section has an inverse dependence on E_R for the hypothetical molecules treated. This suggests that IM reaction cross section data should be analyzed with regard to the effects of rotational energy. Also, ion energy dependencies of such cross sections should be reviewed in the context of the numerical results. More detailed comparisons using typical molecules (rather than hypothetical) are required before the description of these collisions is complete.

Lewis Research Center,
National Aeronautics and Space Administration,
Cleveland, Ohio, November 3, 1965.

APPENDIX A

SYMBOLS

A	rotational constant, $h/8\pi^2 I_A$, sec^{-1}
A_c	collision area in the numerical study, πb^2, cm^2
B	rotational constant, $h/8\pi^2 I$, sec^{-1}
b	classical free particle impact parameter, L/Mv_1, cm; $1Å = 10^{-8}$ cm
b_c	critical impact parameter for IM capture collisions (defines cross section), cm
b_{ci}	numerically calculated critical impact parameter for capture, cm
C	constant appearing in $\bar{\sigma}_{tR}$ expression, $4E_R\alpha_o/\mu^2 = 2E_R/\epsilon_c$, dimensionless
C_R	collision parameter employed in computer study, ratio of number of collisions observed to number of cases tried, dimensionless
E_R	rotational energy of linear molecule, ergs; 1.6×10^{-12} erg = 1 eV
E_{RT}	rotational energy of symmetric top polar molecule, ergs
e	unit electronic charge, 4.8×10^{-10} esu charge units
F	electric field of ion, e/R^2, V/cm; 300 V/cm = 1 esu field unit
F_r	radial component of ionic electric field, V/cm
f(J)	rotational distribution function, probability that the rotator is in interval J to J + dJ at J, dimensionless
h	Planck's constant, 6.63×10^{-27} erg-sec
$\hbar$	$h/2\pi$, 1.1×10^{-27} erg-sec
I	moment of inertia, $(g)(cm^2)$
I_A	moment of inertia about symmetry axis of top, $(g)(cm^2)$
I_B	rigid rod moment of inertia; also larger moment of inertia for prolate symmetric top, $(g)(cm^2)$
J	rotational quantum number, dimensionless
K	projection of J quantum number on symmetry axis of top, dimensionless
k	Boltzmann's constant, 1.38×10^{-16} erg/(^oK)(molecule)
L	classical translational angular momentum, Mv_1b, $(g)(cm^2)/sec$
L_1	Lagrangian function for model I, ergs
L_2	Lagrangian function for model II, ergs
ℓ	variable length of an ion through the target gas, cm
M	reduced mass, $M_{eff} = M_oM_1/(M_1 + M_o)$, g; atomic mass unit (amu) = 1.6×10^{-24} g

M_J projection of rotational quantum number in direction of ion field, dimensionless

M_o mass of polar molecule, g

M_1 mass of ion, g

N_J relative number density of linear rotators that are in J^{th} state with rotational energy, $E_R = J^2\hbar^2/2I$

N_{JK} relative number density of symmetric top rotators that are in a particular state with quantum numbers J and K and rotational energy, $E_{RT} = \frac{J^2\hbar^2}{2I_B} + K^2\left(\frac{\hbar^2}{2I_A} - \frac{\hbar^2}{2I_B}\right)$

P_J probability that rotator is in $\pm M_J^{th}$ state, $1/(J+1)$, dimensionless

P_J' probability that symmetric top is in a state specified by a particular M_J and a particular K, $1/(2J+1)$, dimensionless

Q observed cross section, cm^2

R distance between centers of mass of ion and molecule, cm

R_c distance of closest approach for the effective potential treatment at low ion velocity, cm

R_h hindering distance at which maximum potential interaction is equal to the rotational energy, $(\mu e/E_R)^{1/2}$, cm

R_{REF} reference distance

$\mathcal{R}$ nondimensional distance

T gas temperature of target molecules, ^oK

T_1 kinetic energy term for model I, ergs

T_2 kinetic energy term for model II, ergs

t time, sec

t_c effective collision time, R_h/v_1, sec

t_R characteristic period of rotation for polar molecule, sec

t_{REF} reference time

V_{eff} effective interaction potential for ion-symmetric top system at low ion velocity, ergs

V_{int} total interaction potential, ergs

V_L Langevin polarization potential, ergs

V_P ion-dipole potential term, ergs

V_1 potential energy term for model I, ergs

V_2 potential energy term for model II, ergs

v_{max} upper limit velocity for which quantum mechanical average cross section is valid, cm/sec

v_{min} lowest ion velocity at which sudden approximation is valid, cm/sec

v_1 ion velocity, cm/sec

ΔW_1 first-order Stark interaction energy, ergs

ΔW_{1T} first-order Stark interaction energy for symmetric top, ergs

ΔW_2 second-order Stark interaction energy, ergs

ΔW_{2R} second-order Stark interaction energy for rigid rotator, ergs

ΔW_{2T} second-order Stark interaction energy for symmetric top, ergs

α_{iR} induced polarizability of rigid polar rotator, cm^3

α_o average electronic polarizability of molecular ground state, cm^3

α_{tR} total polarizability of rigid rotator, cm^3

α_{tT} total polarizability of symmetric top molecule, cm^3

ϵ relative (translational) energy of ion molecule pair, ergs

ϵ_c critical relative (translational) energy, $\mu^2/2\alpha_o$, ergs

ϵ_1 translational energy of ion, ergs

η_1 azimuthal angle for rotational motion of rigid rod (model I), rad

η_2 azimuthal angle for rotational motion of the symmetric top (model II), rad

Θ polar angle for translational motion in models I and II, rad

θ angle between ion field F and negative end of dipole, rad

μ permanent dipole moment of polar molecule, esu-cm; 1 Debye unit = 10^{-18} esu-cm

μ_{12} dipole moment matrix element for symmetric top, esu-cm

ξ Euler angle for rotational motion, rad

σ microscopic cross section, cm^2

σ_{ci} numerically calculated collision cross section, πb_c^2, cm^2

σ_{c1} numerically calculated cross section for model I, cm^2

σ_{c2} numerically calculated cross section for model II, cm^2

σ_D maximum ion-permanent dipole contribution to capture cross section, cm^2

σ_{iR} partial cross section for induced polarizability contribution to ion-rigid rotator collision, cm^2

$\bar{\sigma}_{iR}$ average cross section for induced polarizability collision of ion with rigid rotator polar molecule, cm^2

σ_L Langevin cross section, $\pi\left(2\alpha_o e^2/\epsilon\right)^{1/2}$, cm^2

σ_{max} maximum IM capture cross section, $\sigma_D + \sigma_L$, cm^2

σ_{tR} partial cross section for ion-linear molecule capture collision, cm^2

$\overline{\sigma}_{tR}$ average cross section for ion-linear molecule capture collision, cm^2

σ_{tT} partial cross section for ion-symmetric top collision with nonzero electronic polarizability, cm^2

$\overline{\sigma}_{tT}$ average total polarizability cross section for symmetric top, cm^2

σ_{θ} partial cross section for static orientation cross section at high ion velocity, cm^2

$\overline{\sigma}_{\theta}$ static orientation average cross section for high ion velocity, cm^2

τ_R nondimensional time

Φ azimuthal angle for translational motion in models I and II, rad

φ azimuthal angle for spatial integration, rad

ψ_2 coordinate for rotation of symmetric top about the symmetry axis, rad

Ω solid angle, 4π, rad

APPENDIX B

DERIVATIONS OF THE AVERAGE CROSS SECTIONS FOR THE LINEAR MOLECULE WITH ZERO AND NONZERO ELECTRONIC POLARIZABILITY

Zero Electronic Polarizability

At high J the induced polarizability α_{iR} from equation (18) reduces to

$$\alpha_{iR} = \frac{3\mu^2}{4J^2 E_R}\left(M_J^2 - \frac{J^2}{3}\right) \tag{B1}$$

The i^{th} partial cross section for a molecule in the M_J^{th} state is

$$\sigma_{iR} = \pi P_J\left[\frac{2\alpha_{iR}(M_J)e^2}{\epsilon}\right]^{1/2} \tag{B2}$$

The average cross section is the properly normalized sum of the σ_{iR} over the range of M_J values which give positive α_{iR} contributions. This sum can be replaced by an integral for high J since the rotational levels are effectively continuous. The normalization is $2/(2J + 1)$ since α_{iR} depends on M_J^2; this reduces to $1/J$ for high J. The average cross section is then

$$\bar{\sigma}_{iR} = \int_{J/\sqrt{3}}^{J}\left[\frac{\mu^2 e^2\left(3M_J^2 - J^2\right)}{E_R \epsilon}\right]^{1/2} dM_J \tag{B3}$$

Integration with insertion of the limits gives

$$\bar{\sigma}_{iR} = \pi\left(\frac{\mu^2 e^2}{4E_R\epsilon}\right)^{1/2}\left\{\frac{\sqrt{6} - \ln\left(\sqrt{3} + \sqrt{2}\right)}{\sqrt{6}}\right\} \tag{B4}$$

Nonzero Electronic Polarizability

At high J the total polarizability is from equation (18b)

$$\alpha_{tR} = \alpha_o + \frac{3\mu^2}{4J^2 E_R}\left(M_J^2 - \frac{J^2}{3}\right) \tag{B5}$$

The t^{th} partial cross section in the form of equation (19) is

$$\sigma_{tR} = \frac{\pi}{J}\left\{\frac{2e^2}{\epsilon}\left[\alpha_o + \frac{\mu^2}{4E_R J^2}\left(3M_J^2 - J^2\right)\right]\right\}^{1/2} \tag{B6}$$

The average cross section is the integral over contributions corresponding to positive α_{tR}; that is,

$$\sigma_{tR} = \frac{\pi}{J^2}\left(\frac{\mu^2 e^2}{2E_R\epsilon}\right)^{1/2} \int_{M_o}^{J} \left(\frac{4E_R J^2 \alpha_o}{\mu^2} + 3M_J^2 - J^2\right)^{1/2} dM_J \tag{B7}$$

where the factor $P_J = 1/J$ has been included. The limit M_o is either

$$M_o = \frac{J}{\sqrt{3}}\left(1 - \frac{4E_R\alpha_o}{\mu^2}\right) \text{ for } \alpha_o \leq \frac{\mu^2}{4E_R^a}$$

or

$$M_o = 0 \text{ for } \alpha_o \geq \frac{\mu^2}{4E_R^b}$$

The average cross section when the exponent of E_R is a is

$$\bar{\sigma}_{tR} = \pi\left(\frac{3\mu^2 e^2}{2E_R^{\epsilon}}\right)^{1/2}\left[\frac{\sqrt{C+2}}{2\sqrt{3}} + \frac{C-1}{6}\ln\left(\frac{\sqrt{C+2}+\sqrt{3}}{\sqrt{C-1}}\right)\right] \tag{B8a}$$

When the exponent is b, the cross section is

$$\bar{\sigma}_{tR} = \pi\left(\frac{3\mu^2 e^2}{2E_R^{\epsilon}}\right)^{1/2}\left[\frac{\sqrt{C+2}}{2\sqrt{3}} + \frac{C-1}{6}\ln\left(\frac{\sqrt{C+2}+\sqrt{3}}{\sqrt{1-C}}\right)\right] \tag{B8b}$$

APPENDIX C

COORDINATE SYSTEM FOR MODEL I

The coordinate system used to describe the interaction between the ion and the linear polar molecule is shown in figure 9 (p. 23). The polar angle for translational motion Θ defines the orientation of the R vector relative to the z-axis. It is measured from +z to -z as indicated and goes from 0 to π. The azimuthal angle for translation Φ defines the orientation of the projection of R in the x-y plane with respect to the x-axis. This angle is measured counterclockwise and goes from 0 to 2π. The polar angle for rotation ξ_1 defines the orientation of the negative half of the rod with respect to the z-axis. It is measured from +z and ranges from 0 to π. The azimuthal angle for rotation η_1 defines the orientation of the projection of the negative end of the dipole with respect to the x-axis. It is measured in the x-y plane in the counterclockwise direction and ranges from 0 to 2π.

APPENDIX D

CHOICE OF CONSTANTS AND TRANSLATIONAL ENERGY APPROXIMATION

The dipole moment μ is presumed to have a constant value along the internuclear axis equal to a typical value of 1.67 Debye units. The representative value chosen for the electronic polarizability α_o was 1.67 angstroms^3. The moment of inertia I_B employed in model I was 3.85×10^{-38} gram-centimeter^2. This value is 10 times the principal axis moment of inertia for the methyl alcohol molecule CH_3OH (ref. 10).

For convenience, all of the relative translational velocity is assigned to the ion. This is a good approximation down to where the ion has thermal energy. The ion energy $\epsilon_1 = M_1 v_1^2/2$ is simply referred to the center mass by replacing M_1 by the effective mass of the pair M. The relative energy ϵ is merely $Mv_1^2/2$. Many IM systems consist of equal mass molecules and molecular ions where $M = M_1/2 = M_o/2$, the "parent" ion case (refs. 6 and 7). The value of M chosen was 5.12×10^{-23} gram for models I and II.

APPENDIX E

INITIAL CONDITIONS AND EQUATIONS OF MOTION

The initial conditions for variables and their time derivatives were chosen so as to ensure negligible IM interaction at $t = 0$. This had to be done without entailing prohibitive running time on the computer. The initial value of R for all cases was 50 angstroms. Initial values of the four angles Θ, Φ, ξ, and η were varied as dictated by randomizing the rotational plane and rod orientation. The values of the time derivatives were judiciously chosen so as to restrict the translational and rotational energies to values of interest.

The Lagrangian for the ion-linear molecule system is

$$L_1 = T_1 - V_1 = \frac{M}{2}\left(\dot{R}^2 + R^2\dot{\Theta}^2 + R^2 \sin^2\Theta\, \dot{\Phi}^2\right) + \frac{I}{2}\left(\dot{\xi}_1^2 + \dot{\eta}_1^2 \sin^2\xi_1\right) + \frac{\alpha_o e^2}{2R^4}$$

$$+ \frac{\mu e}{R^2}\left\{\cos(\xi_1 - \Theta) - \sin\xi_1 \sin\Theta\left[1 - \cos(\eta_1 - \Phi)\right]\right\} \qquad \text{(E1)}$$

The equations of motion follow from

$$\frac{d}{dt}\left(\frac{\partial L_1}{\partial \dot{q}}\right) - \left(\frac{\partial L_1}{\partial q}\right) = 0 \qquad \text{(E2)}$$

where $q = R_1$, Θ_1, Φ_1, ξ_1, and η_1. The programed equations in the form to be solved for the accelerations are

$$\ddot{R} = R\dot{\Theta}^2 + R^2 \sin^2\Theta\, \dot{\Phi}^2 - \left(\frac{2\mu e}{MR^3}\right)\left\{\cos(\xi_1 - \Theta) - \left[1 - \cos(\eta_1 - \Phi)\right]\sin\xi_1 \sin\Theta\right\} - \frac{2\alpha_o e^2}{MR^5} \qquad \text{(E3)}$$

$$\ddot{\Theta} = \sin\Theta\cos\Theta\, \dot{\Phi}^2 - \frac{2\dot{R}\dot{\Theta}}{R} - \left(\frac{\mu e}{R^2}\right)\cdot \frac{\left\{\cos\Theta \sin\xi_1\left[1 - \cos(\eta_1 - \Phi)\right] - \sin(\xi_1 - \Theta)\right\}}{MR^2} \qquad \text{(E4)}$$

$$\ddot{\Phi} = \frac{(\mu e/R^2)\left[\sin\Theta \sin\xi_1 \sin(\eta_1 - \Phi)\right] - 2MR\dot{\Phi} \sin\Theta(R\dot{\Theta} \cos\Theta + \dot{R} \sin\Theta)}{MR^2 \sin^2\Theta} \tag{E5}$$

$$\ddot{\eta}_1 = -\frac{\left[MR \sin\Theta(2\dot{\Phi}R\dot{\Theta} \cos\Theta + R\ddot{\Phi} \sin\Theta + 2\dot{R}\dot{\Phi} \sin\Theta) + 2I_B\dot{\eta}_1\dot{\xi}_1 \sin\xi_1 \cos\xi_1\right]}{I_B \sin^2\xi_1} \tag{E6}$$

$$\ddot{\xi}_1 = \dot{\eta}_1^2 \sin\xi_1 \cos\xi_1 - \frac{\mu e}{I_B R^2}\left\{\sin(\xi_1 - \Theta) + \left[1 - \cos(\eta_1 - \Phi)\right] \cdot \sin\Theta \cos\xi_1\right\} \tag{E7a}$$

An alternate expression for the $\ddot{\eta}_1$ equation which was used to check equation (E6) is

$$\ddot{\eta}_1 = -2\dot{\eta}_1\dot{\xi}_1 \operatorname{ctn}\xi_1 - \frac{\mu e}{I_B R^2} \cdot \frac{\sin(\eta_1 - \Phi)\sin\Theta}{\sin\xi_1} \tag{E7b}$$

Because of singularities in the coordinate system, an alternate system of equation was written in Cartesian coordinates. The problem was transferred to this second system whenever the singularity was approached in the first system and vice-versa.

The values of constants for which there is meaningful IM interaction can be estimated by nondimensionalization of equation (E1). Let a reference time t_{REF} be $\sqrt{I^2/\mu em}$ and a reference distance R_{REF} be $\sqrt{2I/M}$. Then the nondimensional time and distance are

$$\tau_R = \frac{t}{t_{REF}}$$

$$\mathcal{R} = \frac{R}{R_{REF}}$$

The Lagrangian becomes

$$\overline{L}_1 = \frac{M\mu e}{I}\left\{\left(\dot{\mathcal{R}}^2 + \mathcal{R}^2\dot{\Theta}^2 + \mathcal{R}^2 \sin^2\Theta\,\dot{\Phi}^2\right) + \frac{1}{2}\left(\dot{\xi}_1^2 + \dot{\eta}_1 \sin^2\xi_1\right)\right.$$

$$\left. + \frac{1}{2}\frac{\left(\cos(\xi_1 - \Theta) - \sin\xi_1 \sin\Theta\left[1 - \cos(\eta_1 - \Phi)\right]\right)}{\mathcal{R}^2} + \frac{1}{\mathcal{R}^4}\frac{Me\alpha_o}{8\mu I}\right\} \qquad \text{(E8)}$$

The first three parenthetical terms in braces will be of the same order for R equal to R_{REF} for times of the order of $t = t_{REF}$. The $1/\mathcal{R}^4$ term will be significant under such conditions only if the term $Me\alpha_o/\mathcal{R}^4 8\mu I$ is $\cong 1$. For the chosen values of the molecular constants, R_{REF} is roughly 5 angstroms, that is, several molecular diameters. For the same constants, t_{REF} is approximately 2.5×10^{-13} second, the time required for an ion traveling 10^5 centimeters per second to traverse 2.5 angstroms. For the hypothetical molecule, $Me\alpha_o/8\mu I$ is about 0.04 so the R^{-4} term is equal to unity for $R \cong 2.5$ angstroms.

APPENDIX F

COORDINATE SYSTEM, DEGREE OF FREEDOM CONSIDERATIONS, AND EQUATIONS OF MOTION FOR THE ION-SYMMETRIC TOP INTERACTION

In the ion-symmetric top coordinate system the radius vector R and angles Θ and Φ are defined just as in model I. The angle η_2 is actually measured counterclockwise from the x-axis to the line of nodes (ref. 14), but can be defined as in figure 10. Although the polar angle ξ is identical to ξ_1, it was denoted ξ_2 to avoid confusion. The additional angle ψ_2 defines the orientation of the molecular group CH_3 with respect to the symmetry axis. The angles η_2, ξ_2, and ψ_2 are Euler angles, equivalent to the angles θ, φ, and ψ of reference 14.

The ion-dipole potential is the same as in the linear molecule case since the dipole is assumed to be "frozen" on the symmetry axis of the top. The angle ψ_2 introduces a second moment of inertia I_A about this symmetry axis. The coordinate system is shown for a sample prolate top CH_3CN. The moment of inertia ratio I_A/I_B chosen for the hypothetical molecule was 0.2 (prolate top). The angle ψ_2 was varied randomly for a given orientation of the principal (B) axis as specified by η_2 and ξ_2.

The value of $\dot{\psi}_2$ was varied with $\dot{\eta}_2$, $\dot{\xi}_2$, η_2, and ξ_2 so as to insure equipartition of energy in the molecule. Initial conditions were assigned so that one-third of the rotational energy would be present in each degree of freedom.

The additional degree of freedom introduces the only new energy term in the Lagrangian expression. The Lagrangian is

$$L_2 = T_2 - V_2 = \frac{M}{2}\left(\dot{R}^2 + R^2\dot{\Theta}^2 + R^2 \sin^2\Theta\,\dot{\Phi}^2\right) + \frac{I_B}{2}\left(\dot{\xi}_2^2 + \dot{\eta}_2^2 \sin^2\xi_2\right)$$

$$+ \frac{I_A}{2}\left(\dot{\psi}_2 + \dot{\eta}_2 \cos\xi_2\right)^2$$

$$+ \frac{\mu e}{R^2}\left\{\cos(\xi_2 - \Theta) - \sin\xi_2 \sin\Theta\left[1 - \sin(\eta_2 - \Phi)\right]\right\} + \frac{\alpha_o e^2}{2R^4} \qquad \text{(F1)}$$

The equations of motion for model II are

$$\ddot{R} = R\dot{\Theta}^2 + R \sin^2\Theta \, \dot{\Phi}^2 - \frac{2\mu e}{MR^3} \cdot \left\{\cos(\xi_2 - \Theta) - \left[1 - \sin(\eta_2 - \Phi)\right] \cdot \sin \xi_2 \sin \Theta\right\} - \frac{2\alpha_o e^2}{MR^5} \tag{F2}$$

$$\ddot{\Theta} = \sin \Theta \cos \Theta \, \dot{\Phi}^2 - \frac{2\dot{R}\dot{\Theta}}{R} - \frac{\frac{\mu e}{R^2}\left\{\left[1 - \sin(\eta_2 - \Phi)\right]\cos \Theta \sin \xi_2 - \sin(\xi_2 - \Theta)\right\}}{MR^2} \tag{F3}$$

$$\ddot{\Phi} = \frac{-\left[\frac{\mu e}{R^2} \sin\Theta \sin \xi_2 \cos(\eta_2 - \Phi) + 2MR\dot{\Phi} \sin \Theta(R\dot{\Theta} \cos \Theta + \dot{R} \sin \Theta)\right]}{MR^2 \sin^2\Theta} \tag{F4}$$

$$\ddot{\eta}_2 = \frac{\frac{\mu e}{R^2}\left[\sin \Theta \sin \xi_2 \cos(\eta_2 - \Phi)\right] - 2I_B\dot{\eta}_2\dot{\xi}_2 \sin \xi_2 \cos \xi_2}{I_B \sin^2\xi_2} + \frac{I_A\left[\xi_2(\dot{\psi}_2 + \dot{\eta}_2 \cos \xi_2)\right]}{I_B \sin \xi_2} \tag{F5}$$

$$\ddot{\xi}_2 = \dot{\eta}_2^2 \sin \xi_2 \cos \xi_2 - \frac{\mu e}{I_B R^2}\left\{\sin(\xi_2 - \Theta) + \left[1 - \sin(\eta_2 - \Phi)\right]\sin \Theta \cos \xi_2\right\}$$

$$- \frac{I_A}{I_B} \cdot \left(\dot{\psi}_2\dot{\eta}_2 \sin \xi_2 + \dot{\eta}_2^2 \sin \xi_2 \cos \xi_2\right) \tag{F6}$$

$$\ddot{\psi}_2 = \dot{\eta}_2\dot{\xi}_2 \sin \xi_2 - \ddot{\eta}_2 \cos \xi_2 \tag{F7}$$

To avoid singularity difficulties for the symmetric top, an alternate set of equations was written in a second Euler system. These equations were utilized in the same manner as the Cartesian equations written for model I.

REFERENCES

1. Burton, Milton: Development of Current Concepts of Elementary Processes in Radiation Chemistry. J. Chem. Educ., vol. 36, 1959, pp. 273-278.

2. Boelrijk, N.; and Hamill, W. H.: Effects of Relative Velocity Upon Gaseous Ion-Molecule Reactions; Charge Transfer to the Neopentane Molecule. J. Am. Chem. Soc., vol. 84, no. 5, Mar. 5, 1962, pp. 730-734.

3. Stevenson, D. P.; and Schissler, D. O.: Reactions of Gaseous Molecule Ions with Gaseous Molecules. IV. Experimental Methods and Results. J. Chem. Phys., vol. 29, no. 2, Aug. 1958, pp. 282-294.

4. Gioumousis, George; and Stevenson, D. P.: Reactions of Gaseous Molecule Ions with Gaseous Molecules. V. Theory. J. Chem. Phys., vol. 29, no. 2, Aug. 1958, pp. 294-299.

5. McDaniel, Earl Wadsworth: Collision Phenomena in Ionized Gases. John Wiley & Sons, Inc., 1964, ch. 3, pp. 67-75.

6. Theard, Lowell P.; and Hamill, William H.: The Energy Dependence of Cross Sections of Some Ion-Molecule Reactions. J. Am. Chem. Soc., vol. 84, no. 7, Apr. 5, 1962, pp. 1134-1139.

7. Moran, Thomas F.; and Hamill, William H.: Cross-Sections of Ion-Permanent-Dipole Reactions by Mass Spectrometry. J. Chem. Phys., vol. 39, no. 6, Sept. 15, 1963, pp. 1413-1422.

8. Townes, Charles H.; and Schawlow, A. L.: Microwave Spectroscopy. McGraw-Hill Book Co., Inc., 1955.

9. Kauzmann, W. J.: Quantum Chemistry. Academic Press, Inc., 1956, pp. 526-530.

10. Herzberg, Gerhard: Infrared and Raman Spectra of Polyatomic Molecules. Vol. 2 of Molecular Spectra and Molecular Structure, D. Van Nostrand Co., Inc., 1945.

11. Herzberg, Gerhard: Spectra of Atomic Molecules. Vol. 1 of Molecular Spectra and Molecular Structure, Second ed., D. Van Nostrand Co., Inc., 1950.

12. Messiah, Albert: Quantum Mechanics. Vol. II. North-Holland Pub. Co., 1964, pp. 740-744.

13. Bullis, Robert H.: Low Energy Cesium Ion - Atom Collision Cross Section. Report on Thermionic Conversion Specialists Conf., Gatlinburg (Tenn.), Oct. 7-9, 1963, pp. 1-9.

14. Goldstein, Herbert: Classical Mechanics. Addison-Wesley Pub. Co., Inc., 1950, p. 91.

"The aeronautical and space activities of the United States shall be conducted so as to contribute . . . to the expansion of human knowledge of phenomena in the atmosphere and space. The Administration shall provide for the widest practicable and appropriate dissemination of information concerning its activities and the results thereof."

—NATIONAL AERONAUTICS AND SPACE ACT OF 1958

NASA SCIENTIFIC AND TECHNICAL PUBLICATIONS

TECHNICAL REPORTS: Scientific and technical information considered important, complete, and a lasting contribution to existing knowledge.

TECHNICAL NOTES: Information less broad in scope but nevertheless of importance as a contribution to existing knowledge.

TECHNICAL MEMORANDUMS: Information receiving limited distribution because of preliminary data, security classification, or other reasons.

CONTRACTOR REPORTS: Technical information generated in connection with a NASA contract or grant and released under NASA auspices.

TECHNICAL TRANSLATIONS: Information published in a foreign language considered to merit NASA distribution in English.

TECHNICAL REPRINTS: Information derived from NASA activities and initially published in the form of journal articles.

SPECIAL PUBLICATIONS: Information derived from or of value to NASA activities but not necessarily reporting the results of individual NASA-programmed scientific efforts. Publications include conference proceedings, monographs, data compilations, handbooks, sourcebooks, and special bibliographies.

Details on the availability of these publications may be obtained from:

SCIENTIFIC AND TECHNICAL INFORMATION DIVISION

NATIONAL AERONAUTICS AND SPACE ADMINISTRATION

Washington, D.C. 20546